

Cite this: DOI: 10.1039/c1sm06139a

www.rsc.org/softmatter

PAPER

## A viscoelastic regime in dilute hydrophobin monolayers

Elodie Aumaitre,<sup>a</sup> Simon Wongsuwarn,<sup>a</sup> Damiano Rossetti,<sup>b</sup> Nicholas D. Hedges,<sup>b</sup> Andrew R. Cox,<sup>c</sup> Dominic Vella<sup>†d</sup> and Pietro Cicuta<sup>\*a</sup>

Received 16th June 2011, Accepted 11th November 2011

DOI: 10.1039/c1sm06139a

We show unexpected viscoelastic response in dilute conditions for hydrophobin layers subjected to compression in a Langmuir trough. The surface pressure, surface dilatational and shear viscoelasticity, and layer thickness, are probed by combining four different experimental techniques: Wilhelmy plate tensiometry, Surface Quasi-Elastic Light Scattering (SQELS), Surface Shear Rheology and Ellipsometry. At a surface pressure around 6–15 mN m<sup>-1</sup>, the isotherm measured by a Wilhelmy plate displays erratically a kink or small plateau feature. The build up to this point has been probed with SQELS. SQELS data itself require careful interpretation because the Wilhelmy plate measurements cannot be taken as a valid independent measurement of surface pressure for solid-like films. The SQELS raw signal shows a decrease of the capillary wave frequency, while the surface pressure measured by a Wilhelmy plate is still approximately zero. This could be attributed to either an increase of the layer surface pressure not seen by the Wilhelmy plate, and/or to the presence of significant dilatational response; analysis of the SQELS signals indicates a small finite dilatational modulus in the dilute hydrophobin layer. Shear rheology measurements indicate that within this region, the layer acquires some rigidity. Ellipsometry measurements interestingly show that the layer already has a finite thickness in these dilute conditions, and that the thickness increases linearly through the compression until the layer collapses. Combining these elements allows us to develop a clear picture of the build up of surface tension and viscoelasticity within the hydrophobin layer: the layer becomes viscoelastic at pressures which are still negligible. This is consistent with previous reports in the literature of co-existence of condensed and dilute protein domains, if the domain lengthscale is smaller than the area probed by the techniques employed here.

### 1 Introduction

The study of two dimensional films is of great scientific and technological interest, with open problems ranging from understanding the physical properties of biological membranes to tailoring the stability of foams and emulsions. Recently, a protein called hydrophobin, extracted from filamentous fungi, has received much attention. Hydrophobins are able to self-assemble into highly elastic films at water surfaces, that prove to be very effective to stabilise foams and emulsions.<sup>1,2</sup> Amphiphilic layers of macromolecules such as polymers, fatty acids or protein films display rich phase transitions and have been extensively investigated. Phase transitions have been observed in

amphiphilic films, including the transitions between different states of matter in two dimensions: vapour to liquid expanded, liquid expanded to liquid condensed or liquid condensed to solid.<sup>3</sup> Within the more condensed phases, a spectrum of transitions between the two dimensional analogues of various liquid crystalline phases have also been observed.<sup>4</sup> Two dimensional systems can also exhibit a unique two stage melting phenomenon called the Kosterlitz–Thouless transition<sup>5</sup> where an intermediate hexatic phase occurs upon melting; there is evidence that this transition takes place in some Langmuir films.<sup>6</sup>

Practically, amphiphilic films can be formed and studied in a Langmuir trough, where the surface concentration can be controlled, and the viscoelastic properties of the film are probed through the measurement of the surface pressure during compression or expansion of the layer. A widely used and simple way of measuring surface pressure is to dip a Wilhelmy plate into the layer. This method is well established for monolayers in the liquid state. In the case of rigid films the surface tension measured by a Wilhelmy plate can easily provide interesting information,<sup>7</sup> but the recorded values do not necessarily represent the tension of the entire system, and hence have to be interpreted carefully.<sup>8–10</sup>

<sup>a</sup>Cavendish Laboratory, University of Cambridge, JJ Thomson Avenue, CB3 0HE Cambridge, UK. E-mail: pc245@cam.ac.uk

<sup>b</sup>Unilever Discover, Sharnbrook, MK44 1LQ, UK

<sup>c</sup>Centre of Excellence Ice Foods, Unilever, Sharnbrook, MK44 1LQ, UK

<sup>d</sup>ITG, Department of Applied Mathematics and Theoretical Physics, University of Cambridge, Wilberforce Road, Cambridge, CB3 0WA, UK

<sup>†</sup> Present address: OCCAM, Mathematical Institute, 24-29 St Giles', Oxford, OX1 3LB, UK

In previous work<sup>10</sup> we focused on the elastic (solid-like) behavior of hydrophobin layers at high surface coverage. In these conditions, the Wilhelmy plate does not measure a simple surface pressure, but probes instead the stress field of the entire layer. This field is in general complex to calculate, and is affected by the trough geometry, the plate geometry, as well as the viscoelastic properties of the layer. It is therefore desirable to measure the properties of the hydrophobin layer *via* a non-contact probe since this eliminates one boundary condition on the stress field. In addition to its technological interest, the protein hydrophobin provides a challenging elastic system that pushes the boundaries of the current knowledge in surface rheology. Surface waves are spontaneously induced by thermal motion of a fluid surface, and their dynamics contains information on both the tension of the interface and the viscoelastic properties of the layer. The fast dynamics of the liquid fluctuations can be probed non-invasively by light scattering.<sup>11</sup> Surface Quasi-Elastic Light Scattering (SQELS) has emerged as a very useful tool to characterise the surface rheology of Langmuir films, at least in dilute conditions where the effect of the complex compressional modulus has the largest effect on the surface waves.<sup>12,13</sup>

SQELS has proven especially suited to the characterisation of phase transitions. Earnshaw and co-workers<sup>6,14</sup> have studied several phase transitions using SQELS, showing, for a class of systems, that the wave damping coefficient as well as the dilatational modulus show abrupt changes in time. This is characteristic of probing mesoscopic domains of different phases in coexistence with each other and is typical of first order phase transitions, such as the liquid expanded - liquid condensed transition common in many phospholipid monolayers.<sup>4</sup> The equilibrium surface pressure should be equal in the two coexisting phases by definition, but SQELS measurements can access viscoelastic properties at high frequency, which can vary for different co-existing phases.<sup>14</sup> SQELS also enabled the observation of a discontinuous jump in dilatational elastic modulus compared to the equilibrium elastic modulus obtained when the layer enters the hexatic phase.<sup>6</sup> However, Earnshaw's data analysis was based on the Goodrich<sup>15,16</sup> and Kramer<sup>17</sup> model which considers a complex surface tension. This model was extensively used in the literature up to around a decade ago when Buzza *et al.*<sup>18,19</sup> conclusively showed that the imaginary part of the surface tension is unphysical and that wave dynamics should not be over-parametrized. The surface tension measured by light scattering should be the same as the equilibrium value, and any frequency dependence should be accounted for in a frequency dependent dilatational (compressional) modulus. The hydrodynamic theory described by Buzza<sup>19</sup> accounts for a Newtonian fluid covered in a thin layer characterized by a tension and a complex dilatational modulus (*i.e.* elastic and dissipative processes). Layers may be more complex than that, and other processes occurring in the adsorbed layer can potentially lead to abnormalities in the determination of the viscoelastic parameters, such as negative surface viscosities.<sup>20,21</sup> Work by Lopez *et al.*<sup>22</sup> showed that the classic hydrodynamic model fails to determine the surface tension and the shear modulus when domains of different viscoelastic properties coexist. This leads to the measurement of apparent negative surface viscosities. While Buzza's theoretical work has clarified greatly the fitting of the SQELS signal in all cases where the surface tension can be

measured independently,<sup>23,24</sup> for the hydrophobin layer investigated here (and similarly for layers with solid-like properties) it is not possible to take the Wilhelmy plate surface pressure as a valid equilibrium value.<sup>10</sup>

Phase transitions can often result in a dramatic variation of the layer thickness, as observed in the tilting of lipids.<sup>4</sup> Ellipsometry is a very accurate and non-invasive tool to measure the variation in the film thickness. In the case of coexistence of solid and liquid domains, it can also provide rough information on the length-scale of those domains compared to the size of the laser beam.

The subject of this study is the protein hydrophobin HFBII. Although the literature is still scarce on this protein, compression isotherms measured by a Wilhelmy plate have been reported and did not display any signature of a phase transition.<sup>2,25</sup> However, Brewster Angle Microscopy measurements performed on hydrophobin HFBII Langmuir films have shown the presence of micron-sized domains before and around the upturn in surface pressure. Grazing incidence X-ray reflectivity measured a layer thickness of about 24 Å in those same conditions.<sup>26</sup> The viscoelastic properties of hydrophobin HFBII have been the subject of a few studies, reporting exceptionally high dilatational<sup>2</sup> and shear<sup>1,27</sup> moduli.

The present study aims at investigating hydrophobin Langmuir films for dilute concentrations and, in particular, at probing a viscoelastic regime discovered where the Wilhelmy plate indicates a surface pressure around zero. We report Wilhelmy plate measurements in which isotherms have varying shapes; most are completely smooth but a few show a small plateau or kink appearing at different surface pressures. This isotherm feature could be an indication of a first order phase transition in the layer. Surface light scattering probes the dynamics of surface waves. A well defined frequency and damping correspond to each specific wavelength. Data can be analyzed in this way, which is known as "Phenomenological fitting", obtaining frequency and damping parameters. For pure liquid interfaces, the interpretation of the phenomenological parameters is straightforward in terms of the physical properties of the liquid and interface (density, viscosity, surface tension). However in the presence of a surface layer we show that the interpretation of the phenomenological parameters is delicate: at an area per molecule much larger than the upturn of the conventional surface pressure, the capillary wave frequency is observed to fall. It is shown that this fact could equally well be interpreted as an increase in the surface pressure or as an increase of the dilatational modulus. The fitting of the same scattering data using a full hydrodynamic model shows that it is more plausible to attribute this change in the layer dynamics to the onset of viscoelasticity in the film. Surface shear rheology and ellipsometry data confirm that in this pre-upturn region, the layer has already started to develop some rigidity.

## 2 Materials and methods

### 2.1 Hydrophobin

Class II hydrophobin (HFBII) from *Trichoderma Reesei* was a gift from Unilever Global Development Centre and was obtained from VTT Biotechnology (Espoo, Finland). Details of the preparation are described elsewhere.<sup>28,29</sup> The stock solution has a concentration of 7.1 mg ml<sup>-1</sup> and was stored frozen. The

sample can be stored in the fridge during experiments and can sustain multiple thawing/freezing cycles without degrading. Before each experiment, the hydrophobin sample was sonicated for one minute, as in previous work.<sup>10</sup>

## 2.2 Langmuir trough

Multiple droplets, each of volume 1  $\mu\text{L}$ , are deposited gently (using a microsyringe) onto a subphase consisting of de-ionised water (ElgaStat UHQII, Elga Process Water, resistivity of 18  $\text{M}\Omega\text{cm}$ ) contained within a Langmuir trough. This process leads to the formation of a layer where the total amount spread is in the range 12  $\mu\text{g}$  to 110  $\mu\text{g}$ . The Langmuir trough is a model 611 (Nima Technology, Coventry, UK), with maximum length  $L = 30\text{ cm}$  and width  $w = 20\text{ cm}$ . The sample is spread with the barriers fully opened. The layer is then allowed to equilibrate for 20 min after spreading before compression is started. The temperature of the subphase was set to 22  $^{\circ}\text{C}$  and maintained by a cooling bath (BC20, Fisher Scientific). Two computer-controlled barriers allow the symmetrical compression of the layer at a constant speed of 10  $\text{cm}^2\text{min}^{-1}$ . The trough was cleaned thoroughly and a fresh protein layer spread for each run of the experiment because hydrophobin layers undergo irreversible changes after just one compression.

## 2.3 Wilhelmy plate

The surface pressure of a layer is defined to be  $\Pi = \gamma_c - \gamma_{\text{layer}}$ , where  $\gamma_c$  is the surface tension of the clean air–water interface ( $\gamma_c \approx 72\text{ mN m}^{-1}$ ) and  $\gamma_{\text{layer}}$  is the surface tension of the interface covered with protein. The surface pressure is measured using a Wilhelmy plate consisting of a 1 cm wide filter paper hung from a microbalance sensor (type PS4, Nima Technology) with a precision of  $\pm 0.01\text{ mN m}^{-1}$ . The Wilhelmy plate is placed in the centre of the trough, in a vertical position and orientated parallel to the barriers using a specially designed rigid hook. The plate provides reliable measurements only when placed midway between the two barriers; when placed off-axis, asymmetric forces exerted on the plate result in its horizontal displacement, and hence to erroneous measurements. The plate orientation is critical in the measurement of surface pressure in layers with finite shear elasticity.<sup>7</sup>

## 2.4 Surface Quasi-Elastic Light Scattering

The SQELS experimental set up has been described in detail by Cicutta *et al.*<sup>13</sup> Briefly, a laser beam (a 10 mW He–Ne laser, wavelength  $\Lambda = 633\text{ nm}$ , Spectra Physics, USA) passes through a combination of a half wave plate and a polarizing-beamsplitter to control the intensity and the polarization of the incident light. The beam size, profile and collimation are controlled by a spatial filter composed of two microscope objectives and a pinhole. The beam then goes through a weak diffraction grating and a system of two lenses that achieve (a) the convergence of the fan of grating-refracted beams onto the surface of the liquid, and (b) focus of the beam at a plane where a photomultiplier tube is placed. The photon correlation is done in heterodyne mode: one of the beams from the diffraction grating provides a coherent reference source of light. A neutral density filter is added to adjust the intensity of the reference beams relative to the main

beam. The Langmuir trough is placed onto an anti-vibration table (TS-150, HWL Scientific Instruments, Germany) and enclosed in a metal draft-proof enclosure. The entire optical set up is mounted on an optical bench. The reference beam, and a solid-angle section of the light field scattered by the surface are then focused together into a millimetre-sized aperture of a photomultiplier tube. The intensity signal is passed through a discriminator circuit, and analysed by a digital correlator (BI9000, Brookhaven, USA). The result is a temporal auto-correlation function of the amplitude of one mode of the liquid surface roughness. By changing scattering angle  $\Phi$  it is possible to access a wave of different wavelength since  $q = 2\pi/\lambda$ . In the present study, various values of  $q$  were selected, from 150 to 320  $\text{cm}^{-1}$ , and correlator delay times are chosen in the range (10  $\mu\text{s}$  to 2.5 ms). For a given scattering angle  $\Phi$ , the wave vector  $q$  also depends on the incidence angle  $\theta$  and on the laser wavelength (see Fig. 1) according to eqn (1):

$$q = \frac{2\pi}{\lambda} \cos(\Phi)\cos(\theta). \quad (1)$$

While the surface pressure is small, the effect of the surface layer on the SQELS signal is a small perturbation with respect to the signal of a clean interface. The measurement therefore requires calibration of various instrument parameters, which is achieved by acquiring several signals for a clean water surface. Following this, the layer is spread, as described above. Note that the laser beam is delivered to the centre of the trough and that the Wilhelmy plate is not present in these experiments.

With hydrophobin layers, it was found that consistent results are obtained under continuous compression, and isotherms are independent on compression speed in the range accessible by our trough.<sup>10</sup> Therefore, the layers were maintained under slow but steady compression, with barrier speed of 10  $\text{cm}^2\text{min}^{-1}$ . We have checked on pure water surfaces that the movement of the barriers during the compression did not affect the capillary waves. Correlation functions were averaged over 45 s (a time judged to be adequate for the autocorrelation function to have a good signal to noise ratio). Consequently, the resulting data point on

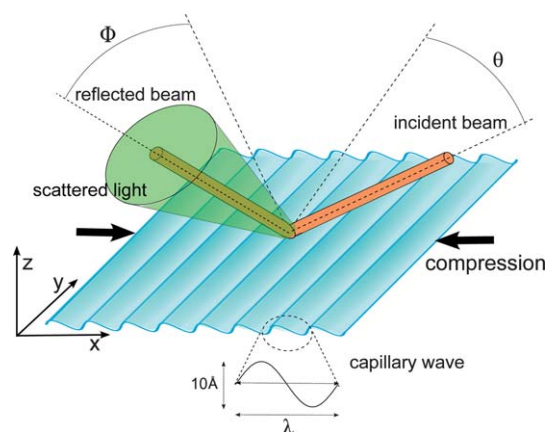


**Fig. 1** Diagram of the trough and beam geometries in the experiment of light scattering from dynamical thermal surface roughness (SQELS). The plane of incidence is  $(x, z)$ , and also includes the specularly reflected beam and the solid angle of scattered light which is selected for acquisition.

an isotherm is to be interpreted as an average value taken while the trough area has changed by 7.5 cm<sup>2</sup>.

The SQELS signal can be fitted using two approaches. The first, which we call “phenomenological”, has the advantage of being very robust: just three physical parameters, wave frequency  $\omega$ , damping  $\Gamma$  and a phase term  $\phi$  (in addition to instrumental parameters) are sufficient to describe the capillary waves of a clean interface (such as water) satisfactorily. The autocorrelation function is given as a function of the delay times  $\tau$  by:

$$C_q(\tau) = B + A \cos(\omega\tau + \phi) \exp(-\Gamma\tau) \exp\left(\frac{-\beta^2\tau^2}{4}\right) + \text{droop}(\tau) + \text{fast afterpulse}(\tau) \quad (2)$$

where the term  $\text{droop}(\tau) = -D\tau^2$  accounts for long time decorrelation due to surface motion, and the term  $\text{fast afterpulse}(\tau) = f_1 \cos(f_2\tau) \exp\left(\frac{-\tau}{f_3}\right)$  accounts for the after-pulse effect typical of the photomultiplier tube used here. The Gaussian term includes the parameter  $\beta$  which accounts for the instrument resolution (broadening of the power spectrum).  $B$  corresponds to the baseline of the signal, and  $A$  to the amplitude of the oscillations. For a clean interface, there is a classical result obtained by Kelvin for inviscid fluids: the surface tension  $\gamma$  can be calculated from the frequency  $\omega$ , the wave vector  $q$  and the density of the subphase  $\rho$  using the dispersion relation:<sup>12</sup>

$$\gamma = \frac{\omega^2 \rho}{q^3}. \quad (3)$$

Eqn (3) is the zero order term neglecting the viscosity of the liquid, and is already imprecise for a low viscosity liquid such as water, see ref. 30 for a recent overview on this point.

If there is a film spread or adsorbed on the surface, then in most cases this will have viscoelastic response (and usually the compressional character dominates over the shear response), then the properties of the longitudinal waves will be modified. Although in practice the phenomenological equation eqn (2) still provides an adequate and robust fit of the data, its drawback is that it is not straightforward to recover the surface physical properties. In particular, the surface pressure cannot then be calculated using eqn (3). In the presence of a surface layer, the in-plane (dilatational and shear) and out-of-plane (capillary) motions act as coupled oscillators, and so resonate when their frequencies match. In the dilute regime studied in the present experiment, we assume that the shear modulus is negligible compared to the dilatational modulus. The SQELS signal probes the properties of the capillary waves. These properties are maximally affected by the dilatational properties close to the resonance condition, which occurs<sup>11</sup> when  $\varepsilon/\gamma = 0.16$ . This coupling therefore allows, at least in principle, for the characterisation of the complex dilatational modulus.

A hydrodynamic model including the presence of the elastic layer was developed by Lucassen and van den Tempel<sup>31</sup> and is described by Langevin and Bouchiat in the context of light scattering from thermal waves:<sup>11,32</sup> the power spectrum  $P_q(\omega)$  of the scattered light is related to the surface wave dispersion relation  $D(\omega)$ , which now contains the dilatational modulus  $\varepsilon^* = \varepsilon' + i\omega\eta_d$ . The time autocorrelation measured by the correlator is:

$$C_q(\tau) = B + A F.T.[P_q(\omega)] \exp\left(\frac{-\beta^2\tau^2}{4}\right) + \text{droop}(\tau) + \text{fast afterpulse}(\tau) \quad (4)$$

where  $F.T.$  is the Fourier transform of the power spectrum  $P_q(\omega)$  and:

$$P_q(\omega) = \frac{k_B T}{\pi\omega} \text{Im} \left[ \frac{i\omega\eta(m+q) + \varepsilon^* q^2}{D(\omega)} \right],$$

with  $m = \sqrt{q^2 + i\frac{\omega\rho}{\eta}}$ ,  $\text{Re}(m) > 0$  and

$$D(\omega) = [\varepsilon^* q^2 + i\omega\eta(q+m)] \left[ \gamma q^2 + i\omega\eta(q+m) - \frac{\rho\omega^2}{q} \right] - [i\omega\eta(m-q)]^2. \quad (5)$$

In practice, before spreading hydrophobin, ten signals were acquired for 45 s each on the pure water subphase. This allows for the determination of the wave vector  $q$ , the properties of the after-pulse  $f_2$  and  $f_3$ , and the instrument resolution  $\beta$ . For the experiment reported here, the instrumental resolution  $\beta$  has a value of  $1106 \pm 37 \text{ s}^{-1}$  and the wave vector  $q$  is  $157.4 \pm 0.05 \text{ cm}^{-1}$ . The viscosity  $\eta$  and density  $\rho$  of the subphase are obtained from literature values for water. These values are subsequently kept fixed for the fitting of the signals in the presence of the hydrophobin layer. Buzza *et al.*<sup>18</sup> have shown that the equilibrium surface tension can be used in the hydrodynamic fitting, hence only the elastic and viscous parts of the dilatational modulus are fitted. The equilibrium surface tension can usually be measured by performing very slow compression in a Langmuir trough. However, a previous study on hydrophobin layers<sup>10</sup> has shown that Wilhelmy plate measurements do not give a value of the pure equilibrium surface tension. Consequently, the surface tension was not fixed in the data analysis but was an additional parameter to fit. All the data were fitted using the minimisation routines Minuit developed at CERN,<sup>33</sup> interfaced with Matlab to provide a minimisation package “fminuit”.<sup>34</sup> The fitting of the autocorrelation signals using the full hydrodynamic model is shown in Fig. 2.

## 2.5 Shear rheology

The complex shear modulus was recorded by a du Noüy ring (1.2 cm diameter) oscillating in plane. The ring is placed at the liquid surface in the centre of the trough during compression. The ring is connected to a CIR-100 instrument (Camtel, UK), which relies on the “normalized resonance” technique. Combined with a sensitive transducer, this instrument allows the measurement of very small stresses and is particularly adapted to probe the onset of the shear modulus. The instrument then saturates when the shear modulus reaches quite modest values (several tens of  $\text{mN m}^{-1}$ ). The oscillation frequency was set to 2 Hz and the angular amplitude was 8 mrad. Spigone *et al.*<sup>35</sup> have shown that positioning a confinement ring around the du Noüy ring helps defining the shear strain field. However, in our case, the rigidity of the hydrophobin layer might prevent it from flowing into the confinement ring. Consequently, we did not place any confinement ring and the resulting values of shear moduli are therefore qualitative.

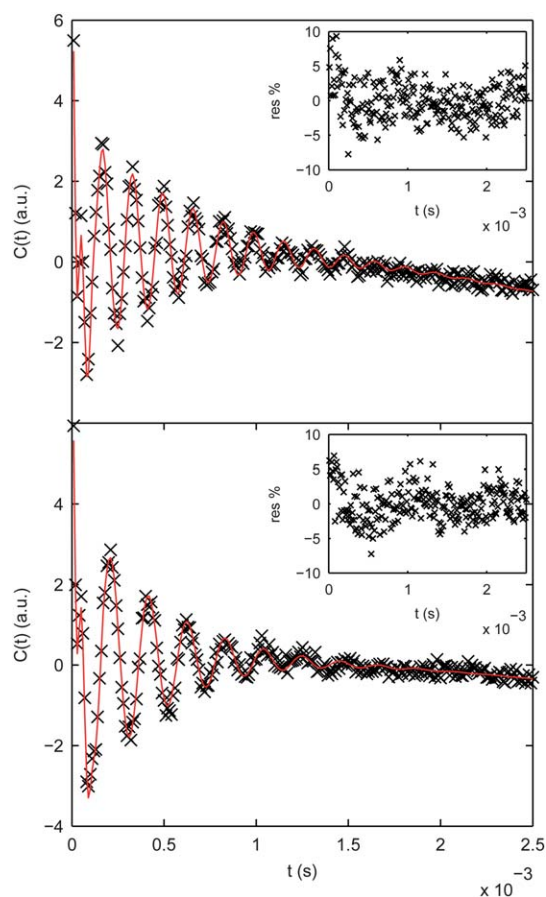


**Fig. 2** The autocorrelation signals (x) are fitted using the full hydrodynamic model of eqn (4) (solid line). Prior to fitting, the average value of the signal was subtracted. The signals shown here were recorded at  $q = 274.2 \text{ cm}^{-1}$ , for surface concentrations of 1.23 and  $2.02 \text{ mg m}^{-2}$  and surface pressures of 0.5 and  $21.7 \text{ mN m}^{-1}$  for the top and bottom graphs respectively. The inset graphs show that the residuals after fitting stay below 10%, which corresponds to a satisfactory fit.

## 2.6 Ellipsometry

By mounting an ellipsometer onto a Langmuir trough, one can follow accurately the evolution of the film thickness as the layer is compressed. The measurements of the two angles  $\Delta$  and  $\Psi$  were performed by null ellipsometry using the Multiskop (Optrel GbR) ellipsometer at a single wavelength  $\lambda = 638 \text{ nm}$  with an angle of incidence of  $45^\circ$ . The Langmuir trough used for the ellipsometry measurements was a custom-made trough with dimensions of  $26 \times 8.6 \text{ cm}^2$ , the electronics controlling the trough were purchased from Riegler&Kirstein (Germany). The surface pressure was recorded with a 1cm-wide filter paper Wilhelmy plate placed in the centre of the trough. The ellipsometry signal was recorded about 4 cm away from the Wilhelmy plate in the  $x$  direction (Fig. 1). The amount of hydrophobin spread was varied from  $19.9 \mu\text{g}$  to  $27 \mu\text{g}$  to match the range of surface concentrations in the experiments performed on the larger Nima 611 trough. The exact value of the film thickness was not calculated since the refractive index of hydrophobin films was not known. A detailed study of the hydrophobin Langmuir film thickness has been undertaken by Kisko *et al.*<sup>26</sup> Nevertheless, the evolution of the phase angle  $\Delta$  upon compression can provide

qualitative data on the film thickness since  $\Delta$  is directly proportional to the thickness.

## 3 Results

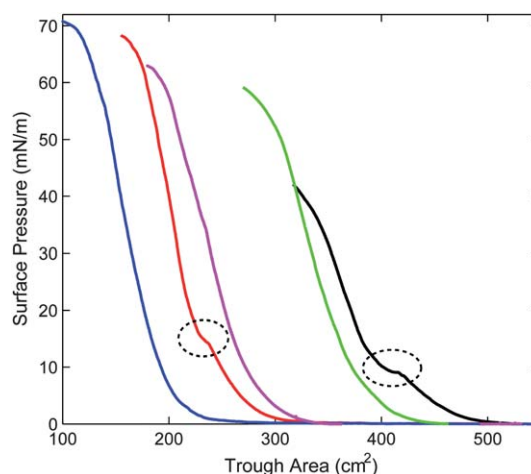
### 3.1 Surface pressure measurements by Wilhelmy plate

Fig. 3 shows a selection of isotherms of compression of hydrophobin Langmuir films, measured using a Wilhelmy plate. Around one hundred isotherms have been measured, each from a freshly spread layer. While some isotherms display a kink or even a short plateau at a surface pressure of around  $6\text{--}15 \text{ mN m}^{-1}$ , most isotherms appear completely smooth. Protein surface unfolding could potentially explain the difference between the isotherms at different surface concentrations. Hydrophobin, however, shows no evidence of unfolding at surfaces,<sup>36</sup> probably thanks to its rigid native structure exhibiting an external hydrophobic patch and maintained by several disulphide bridges.

Several studies have raised questions about the actual quantity measured by the Wilhelmy plate when the Langmuir layer possesses some rigidity.<sup>9,10</sup> The uncertain interpretation of the Wilhelmy plate data motivated us to repeat the measurement using Surface Quasi-Elastic Light Scattering to probe the variation of surface pressure in the layer.

### 3.2 Surface pressure measurements by Surface Quasi-Elastic Light Scattering

Phenomenological fitting using eqn (2) is highly sensitive to changes of the surface waves frequency. Fig. 4 shows the variation of the three parameters frequency  $\omega$ , damping  $\Gamma$  and phase  $\phi$  during an isotherm of compression. One measure of surface pressure by Wilhelmy plate is shown to facilitate the discussion. The damping coefficient presents a peak which correspond to the maximum coupling between the in-plane and out-of-plane waves.<sup>37</sup> The frequency first decreases with the surface



**Fig. 3** Isotherms of compression measured by a Wilhelmy plate for  $42.6 \mu\text{g}$  (blue),  $59.3 \mu\text{g}$  (red),  $63.9 \mu\text{g}$  (magenta),  $99.4 \mu\text{g}$  (green) and  $106.5 \mu\text{g}$  hydrophobin spread (black). Some isotherms present a plateau or a kink at low surface pressures (below  $15 \text{ mN m}^{-1}$ ). The dependence of isotherm shape on the amount spread was the subject of a previous study.<sup>10</sup>

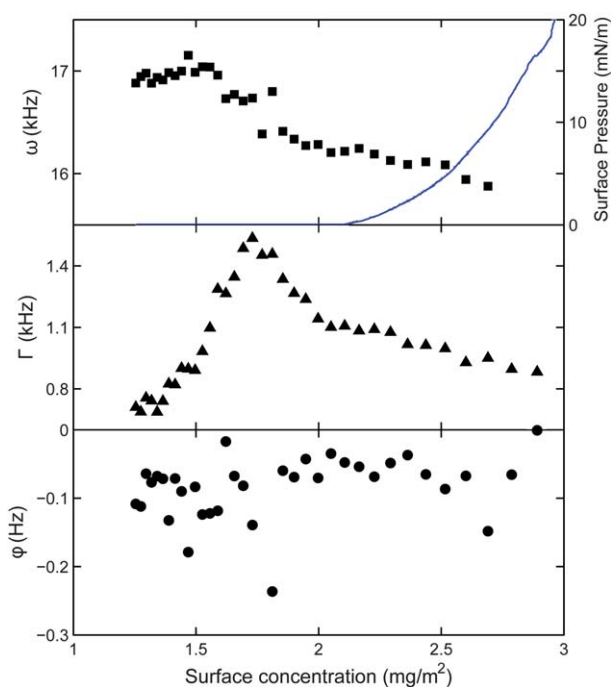


**Fig. 4** Variation of the three parameters: frequency  $\omega$ , damping  $\Gamma$  and phase  $\phi$ , resulting from the phenomenological model of SQELS data. The continuous line on the top graph corresponds to an isotherm of compression measured by a Wilhelmy plate. The wave vector  $q$  was set at  $158.2 \text{ cm}^{-1}$  and the amount of hydrophobin spread was  $63.9 \mu\text{g}$  during this experiment.

concentration before presenting a plateau between 1.6 and  $1.8 \text{ mg m}^{-2}$ , whereas the surface pressure as measured by the Wilhelmy plate remains null. The presence of a plateau could indicate the co-existence of condensed and liquid domains. We should emphasise here that a decrease in the wave frequency does not necessarily indicate an increase of surface pressure (as eqn (3) would suggest) but could also be the signature of an increase in the dilatational modulus. The SQELS data were thus also fitted using the full hydrodynamic model (eqn (4)) which takes into account the coupling between the dilatational waves and the capillary waves. The increased number of fitting parameters makes this a less robust procedure compared to the phenomenological fit: the optimisation routine can get trapped in local minima that may not correspond to physically meaningful values. For example, negative surface pressure or very high values of dilatational modulus (above  $1000 \text{ N m}^{-1}$ ) are not realistic. The Fminuit package makes it possible to fix boundaries on the fitting parameters. The surface pressure was therefore fixed to lie between 0 and  $72 \text{ mN m}^{-1}$  and the elastic and viscous parts of the dilatational modulus were set between  $-1$  and  $1 \text{ N m}^{-1}$  in order to guide the optimization routine towards meaningful solutions.

Fig. 5 compares the result of the full hydrodynamic SQELS fitting with the isotherm measured by a Wilhelmy plate. In the region where the frequency presents a plateau, the full hydrodynamic model suggests that the surface pressure remains null while the dilatational modulus starts to increase. The elastic part  $\epsilon'$  is the first to lift off, reaching modest values around  $17 \text{ mN m}^{-1}$ . This is followed by an increase of the viscous part  $\eta_d$  up to

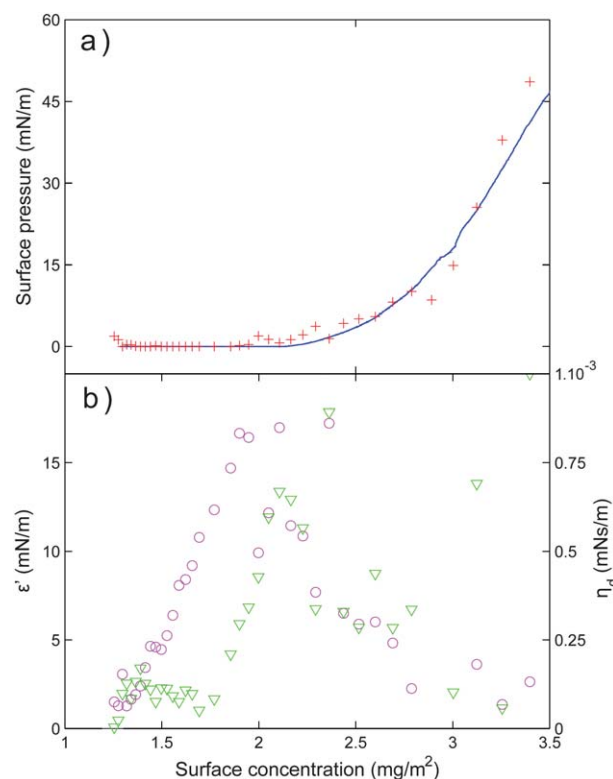


**Fig. 5** (a) Isotherms of compression showing the surface pressure resulting from the full hydrodynamic (+) fittings of SQELS signals. The blue curve shows the isotherm obtained from the Wilhelmy plate, at the same spreading concentration. (b) Values of the elastic part  $\epsilon'$  (○) and the viscous part  $\eta_d$  (▽) of the complex dilatational modulus were also deduced from the full hydrodynamic model. The wave vector  $q$  was set at  $158.2 \text{ cm}^{-1}$  and the amount of hydrophobin spread was  $63.9 \mu\text{g}$ .

$6.7 \times 10^{-7} \text{ N s m}^{-1}$ . At surface concentration higher than  $2.2 \text{ mg m}^{-2}$ , the dilatational modulus becomes large enough to reach the sensitivity of the SQELS technique. It is then not possible to probe the dilatational modulus of the hydrophobin layer once entered this rigid regime. The interpretation of the SQELS data fitting is reviewed in the Discussion section in the light of additional experimental evidence to be presented first.

### 3.3 Shear rheology

Shear rheology measurements were performed to find out at which surface concentration the hydrophobin layer acquires some rigidity. The frequency set in the shear rheology experiments ( $2 \text{ Hz}$ ) is very different than the range explored by SQELS (from  $20$  to  $40 \text{ kHz}$ ) and their results can not be compared directly. However the du Noüy ring experiments provide quantitative information on the onset of the layer elasticity. Fig. 6 shows that the elastic and viscous parts of the complex shear modulus increases slightly from  $2$  to  $2.5 \text{ mg m}^{-2}$  to reach a small but significant value of  $7 \text{ mN m}^{-1}$ . At  $2.5 \text{ mg m}^{-2}$ , the shear modulus increases dramatically. This point corresponds to the end of the plateau where the surface pressure clearly increases and might be an indication of the close-packing of the hydrophobin molecules. These measurements suggest that the

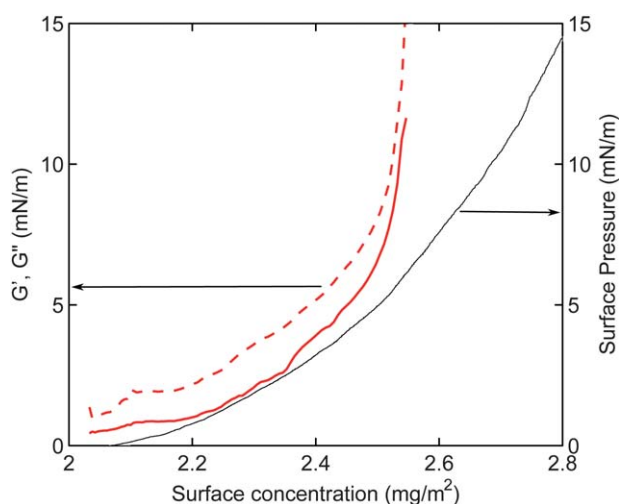


**Fig. 6** The elastic part  $G'$  (continuous red curve) and the viscous part  $G''$  (dashed red curve) of the shear modulus starts to increase at the onset of surface pressure (recorded by a Wilhelmy plate, black continuous curve). This smooth slow build up is followed by a sharp increase at around  $2.5 \text{ mg m}^{-2}$  before instrument saturation. The amount of hydrophobin spread was  $63.9 \mu\text{g}$ .

hydrophobin layer has started to develop some modest shear properties already in the ‘plateau’ region.

### 3.4 Ellipsometry

Fig. 7 shows that the phase angle  $\Delta$  has a finite value when the Wilhelmy plate still indicates  $\Pi = 0 \text{ mN m}^{-1}$  and increases slightly as the layer is being compressed. The signal does not present any abrupt change in the thickness, so we can exclude the formation of mesoscopic domains of different molecular tilt. The dramatic drop in the signal occurring at around  $2.8 \text{ mg m}^{-2}$  corresponds to the appearance of out of plane wrinkles which

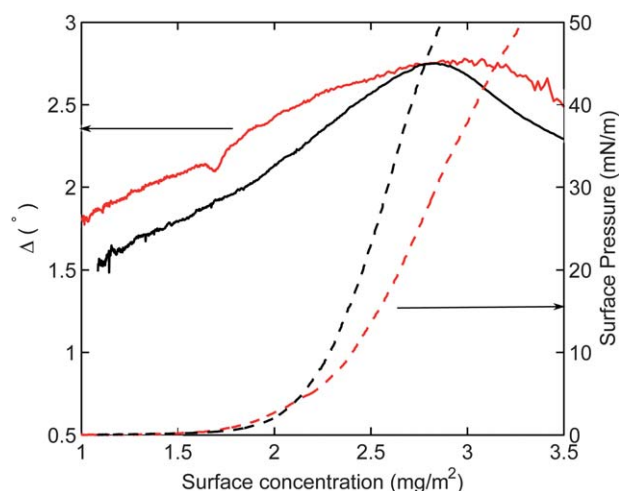


**Fig. 7** The phase angle  $\Delta$  (continuous curve) possesses a finite value at zero surface pressure (recorded by a Wilhelmy plate, dashed curve) and increases linearly upon compression until collapse. The two data sets shown correspond to different amounts of hydrophobin spread:  $19.9 \mu\text{g}$  (red) and  $25.5 \mu\text{g}$  (red).

scatter light in all directions. These data are in agreement with the Brewster Angle Microscopy measurement carried out by Kisko *et al.*,<sup>26</sup> which present small crystalline domains even at  $\Pi = 0 \text{ mN m}^{-1}$  followed by a continuous increase in brightness (proportional to the layer thickness) until  $\Pi = 30 \text{ mN m}^{-1}$ . The layer imaging and thickness measurements<sup>26</sup> show that at very low surface pressure, the hydrophobin HFBII layer already presents a co-existing phase with micron-sized crystalline domains in a liquid matrix which gradually evolves to a pure condensed phase upon compression.

## 4 Discussion

The uncertainties of the SQELS data analysis revolve around the interpretation of the ‘plateau region’. We had to turn to different techniques to obtain clues on the state of the hydrophobin layer in this pressure region. The oscillatory du Noüy ring surface rheometer records a small but significant shear modulus in this region, indicating the increase of the layer rigidity. The ellipsometry data indicate that the layer has a finite and growing thickness, which is more than half of its maximum thickness. This probably would not be the case if the layer were gaseous or liquid. These experimental results indicate that the layer develops some viscoelasticity when the concentration reaches values of  $\sim 1.6 \text{ mg m}^{-2}$ . The viscoelasticity of the layer should therefore be taken into account in the fitting of the SQELS data. The full hydrodynamic fitting indicates that the variation of the capillary waves frequency should be attributed to an increase of the dilatational modulus while the surface pressure remains very low. The hydrophobin layer eventually develops a very high dilatational and shear modulus, whilst the sensitivity of the SQELS technique is limited to dilatational moduli below around  $10 \text{ mN m}^{-1}$ . Other techniques such as bubble tensiometry could complement the information obtained from the SQELS data for regions of higher dilatational modulus. However, it is worth emphasising here that SQELS provides a very sensitive technique to probe the dilute regions, with low but finite viscoelastic properties.

To understand further the impact of a variation of surface pressure coupled with dilatational modulus on the phenomenological and the full hydrodynamic fitting, we generated ‘artificial’ signals using eqn (4). These model signals were then fitted using the phenomenological fitting (eqn (2)) to see the effect on the frequency (which is approximately inversely proportional to the surface pressure for clean interfaces, eqn (3)). More details on this control procedure can be found in Appendix 1. The results clearly show that an increase of the dilatational modulus at constant surface pressure leads to a plateau in the wave frequency. The height of the plateau depends only on the value of the real surface pressure. This indicates that the surface pressure in the concentration region of  $1.6\text{--}2.2 \text{ mg m}^{-2}$  is still very low and that the dilatational moduli have reached values of several tenths of  $\text{mN m}^{-1}$ . Apart from the interpretation of the scattering signal as due to the co-existence of small domains of different viscoelasticities in the dilute region, we have found that a wave frequency plateau is a general feature of the ‘phenomenological fitting’ when there is an increase of the dilatational modulus while the surface pressure remains close to zero.

The presence of viscoelasticity at low concentration is a striking property of hydrophobin films. Future investigations should aim to study the stability of this structure as a function of physico-chemical environment, and also to characterise the frequency dependence of the rheological response. SQELS measurements can only probe a limited ( $q$ ,  $\omega$ ) range, and the technique of electrocapillary excited waves (ECW) seems particularly appropriate to extend these measurements to lower frequency.

## 5 Conclusion

Surface Quasi-Elastic Light Scattering is a useful technique on rigid monolayers such as hydrophobin, as it presents a non-perturbative alternative to Wilhelmy plate measurements. However, the signals obtained experimentally are notoriously difficult to interpret, in particular if the surface tension is not known independently, as is the case here. By comparing several experimental techniques, we believe that we have obtained a clear picture of the behaviour of hydrophobin HFBII in the dilute region. This leads to confident interpretation of SQELS data in a complex system presenting variations of dilatational modulus followed by an increase in surface pressure. We found a previously unreported build-up of the rigidity of the layer, while the surface tension remains very low and where liquid and condensed domains might co-exist. The lengthscale of the domains is likely to be much smaller than the size of the Wilhelmy plate (centimetres) or the area illuminated by the laser (a few millimetres). A possible scenario is that the liquid domains will give place to the most condensed phase upon compression until the jamming point, signified by a sharp increase in both the surface pressure and the viscoelasticity of the layer.

## Appendix 1: Simulating SQELS data

To understand further the parameters resulting from the phenomenological and full hydrodynamic models, we generated model SQELS signals by inputting reasonable values of surface tension  $\gamma$  and dilatational modulus  $\epsilon'$ ,  $\eta_d$  into the full hydrodynamic eqn (4). The droop and after-pulse terms were ignored in our model signals. The elastic and viscous parts of the dilatational modulus were arbitrarily set to similar values ( $\epsilon' = \eta_d \cdot 10^6$ ) for the sake of simplicity. The signals generated were then fitted using the phenomenological model (eqn (2)) to see the effect on the frequency  $\omega$ . The frequency is related monotonically to what one could call an "apparent surface tension" obtained from the Kelvin relation eqn (3). It is worth calculating this apparent surface tension change, as the three parameters  $\gamma$ ,  $\epsilon'$  and  $\eta_d$  are varied, to understand issues of sensitivity. As shown in more detail in ref. 13, one can estimate the values of physical parameters that can be measured realistically, by knowing the typical precision of measuring  $\omega$ . Vice versa, it should be possible to monitor a change of physical parameters that results in a significant change in  $\omega$ .

Fig. 8 shows the effect on the apparent surface tension deduced from the phenomenological fitting when the surface pressure and the dilatational modulus were increased. We can see that when the surface pressure was fixed at 0 mN m<sup>-1</sup> and the dilatational modulus increased, the apparent surface pressure resulting from

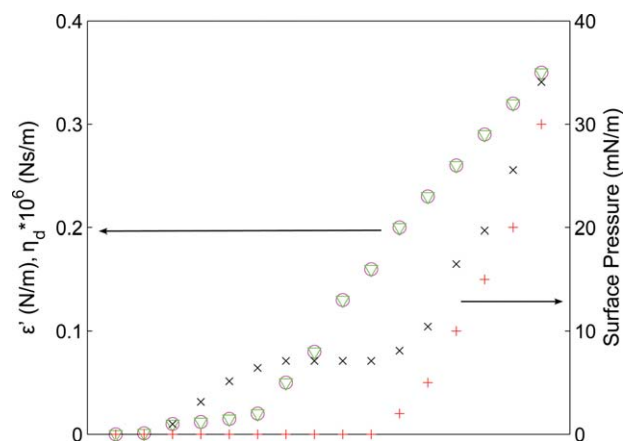


**Fig. 8** Result of the apparent surface pressure after phenomenological fitting ( $\times$ ) on data modelled from the full hydrodynamic equations where values of surface pressure ( $+$ ) and the elastic part  $\epsilon'$  ( $\circ$ ) and viscous  $\eta_d$  ( $\nabla$ ) of the dilatational modulus were specified.

the phenomenological fit first increased before reaching a plateau at around 7 mN m<sup>-1</sup>. This matches what is observed with the phenomenological fitting of SQELS data for the hydrophobin layer (see Fig. 4), with the plateau in the frequency. Fig. 8 also shows that if we impose an increase in the surface pressure, then the apparent surface pressure increases in a similar fashion, and these two values tend to converge indicating that the signal becomes insensitive to the layer's dilatational properties, as described in the text. By varying values of surface pressure, we tested that at a constant surface pressure, the increase in dilatational modulus always leads to a plateau of the frequency (*i.e.* also the apparent surface pressure), the height of the plateau depending on the given surface pressure.

The residual after the phenomenological fitting remains below 2%. The validity of this method was also checked by looking at the difference in the surface pressures when the dilatational modulus was set to 0. We found that the measure of the surface pressure through the phenomenological fit and eqn (3) overestimates the value input into the full hydrodynamic model by about 0.7 mN m<sup>-1</sup>. This is due to the simple formula of eqn (3) being the zero order term in an expansion for small viscosity.<sup>30</sup>

## Acknowledgements

EPSRC and Unilever plc. have funded this project through a CASE award. D.V. was supported by an Oppenheimer Early Career Research Fellowship. P.C. is supported by the Marie Curie Training Network ITN-COMPLOIDS (FP7-PEOPLE-ITN-2008 No. 234810). The ellipsometry experiments were carried out in the Department of Physics of the University of Parma with the kind help of Davide Orsi and Luigi Cristofolini, who we also thank for useful discussions. We thank Unilever Global Development Centre for the gift of hydrophobin.

## References

- 1 A. R. Cox, F. Cagnol, A. B. Russell and M. J. Izzard, *Langmuir*, 2007, **23**, 7995–8002.
- 2 T. B. J. Blijdenstein, P. W. N. de Groot and S. D. Stoyanov, *Soft Matter*, 2010, **6**, 1799–1808.

- 3 G. Gaines, *Insoluble monolayers at liquid-gas interfaces*, Interscience Publishers, 1966, p. 46.
- 4 V. M. Kaganer, H. Mohwald and P. Dutta, *Rev. Mod. Phys.*, 1999, **71**, 779–819.
- 5 J. M. Kosterlitz and D. J. Thouless, *J. Phys. C: Solid State Phys.*, 1973, **6**, 1181–1203.
- 6 D. Sharpe, J. C. Earnshaw, K. Haig and Y. Li, *Phys. Rev. B: Condens. Matter*, 1997, **55**, 6260–6264.
- 7 P. Cicuta and E. M. Terentjev, *Eur. Phys. J. E*, 2005, **16**, 147–158.
- 8 P. Cicuta and D. Vella, *Phys. Rev. Lett.*, 2009, **102**, 138302.
- 9 T. A. Witten, J. Wang, L. Pocivavsek and K. Y. C. Lee, *J. Chem. Phys.*, 2010, **132**, 046102.
- 10 E. Aumaitre, D. Vella and P. Cicuta, *Soft Matter*, 2011, **7**, 2530.
- 11 D. Langevin, *J. Colloid Interface Sci.*, 1981, **80**, 412–425.
- 12 D. Langevin, *Light Scattering by Liquid Surfaces and Complementary Techniques*, Marcel Dekker Inc., 1992.
- 13 P. Cicuta and I. Hopkinson, *Colloids Surf., A*, 2004, **233**, 97–107.
- 14 P. J. Winch and J. C. Earnshaw, *J. Phys.: Condens. Matter*, 1989, **1**, 7187–7205.
- 15 F. Goodrich, *Proc. R. Soc. London, Ser. A*, 1961, **260**, 490.
- 16 F. Goodrich, *Proc. R. Soc. London, Ser. A*, 1981, **374**, 341.
- 17 L. Kramer, *J. Chem. Phys.*, 1971, **55**, 2097.
- 18 D. M. A. Buzza, J. L. Jones, T. C. B. McLeish and R. W. Richards, *J. Chem. Phys.*, 1998, **109**, 5008–5024.
- 19 D. M. A. Buzza, *Langmuir*, 2002, **18**, 8418–8435.
- 20 J. Giermanska-Kahn, F. Monroy and D. Langevin, *Phys. Rev. E: Stat. Phys., Plasmas, Fluids, Relat. Interdiscip. Top.*, 1999, **60**, 7163–7173.
- 21 A. J. Milling, R. W. Richards, R. C. Hiorns and R. G. Jones, *Macromolecules*, 2000, **33**, 2651–2661.
- 22 J. M. Lopez, M. J. Vogel and A. H. Hirska, *Phys. Rev. E: Stat., Nonlinear, Soft Matter Phys.*, 2004, **70**, 056308.
- 23 P. Cicuta and I. Hopkinson, *J. Chem. Phys.*, 2001, **114**, 8659.
- 24 P. Cicuta and I. Hopkinson, *Europhys. Lett.*, 2004, **68**, 65–71.
- 25 A. Paananen, E. Vuorimaa, M. Torkkeli, M. Penttil, M. Kauranen, O. Ikkala, H. Lemmetyinen, R. Serimaa and M. B. Linder, *Biochemistry*, 2003, **42**, 5253–5258.
- 26 K. Kisko, G. R. Szilvay, E. Vuorimaa, H. Lemmetyinen, M. B. Linder, M. Torkkeli and R. Serimaa, *Langmuir*, 2009, **25**, 1612–1619.
- 27 M. J. Berry, D. J. Cebula, A. Cox, M. Golding, R. Keenan, M. Malone and S. Twigg, Aerated food products containing hydrophobin, EP 1623631 B1, 2007.
- 28 M. J. Bailey, S. Askolin, N. Horhammer, M. Tenkanen, M. Linder, M. Penttila and T. Nakari-Setala, *Appl. Microbiol. Biotechnol.*, 2002, **58**, 721–727.
- 29 M. Linder, K. Selber, T. Nakari-Setala, M. Qiao, M.-R. Kula and M. Penttila, *Biomacromolecules*, 2001, **2**, 511–517.
- 30 F. Behroozi, J. Smith and W. Even, *Am. J. Phys.*, 2010, **11**, 78.
- 31 J. Lucassen and M. van den Tempel, *Journal Of Colloid And Interface Science*, 1972, **41**, 491–498.
- 32 D. Langevin and M. Bouchiat, *Comptes Rendus Acad. Sci*, 1971, **272B**, 1422.
- 33 F. James, *MINUIT, Function Minimization and Error Analysis*, <http://wwwasdoc.web.cern.ch/wwwasdoc/minuit/>.
- 34 G. Allodi, *FMINUIT, a Fitting and Optimization Routine*, <http://www.fis.unipr.it/giuseppe.allodi/Fminuit/>.
- 35 E. Spigone, G. Y. Cho, G. G. Fuller and P. Cicuta, *Langmuir*, 2009, **25**, 7457–7464.
- 36 S. Askolin, M. Linder, K. Scholtmeijer, M. Tenkanen, M. Penttil, M. L. de Vocht and H. A. B. Wsten, *Biomacromolecules*, 2006, **7**, 1295–1301.
- 37 R. A. L. Jones and R. W. Richards, *Polymers at Surfaces and Interfaces*, Cambridge University Press, Cambridge, UK, 1999.